doi:10.3788/gzxb20154408.0806005

基于级联直径蚀刻光纤声光光栅的双波长可调谐滤波器

贾洁,冯选旗,张尧,齐新元,贺庆丽,白晋涛
(西北大学 物理学院,西安 710069)

摘 要:提出级联直径蚀刻光纤法实现双波长滤波器的动态调节.采用耦合模理论和分段传输矩阵法进行理论推导和仿真,研究级联声光光栅可调双波长的直径蚀刻光纤滤波器,分析光纤蚀刻对声光光栅传输谱中旁瓣效应的抑制效果.结果表明光纤蚀刻法可以有效抑制旁瓣效应,旁瓣比从0.265下降到0.031;通过调节级联光栅的间隔保证双波长滤波器的两个对称谐振损耗峰的稳定性,间隔增加时左谐振波长峰值减小,右谐振波长峰值增大;双谐振峰的谐振波长由声频信号的频率和光纤级数调节,波长随周期变大而增大,在 270 μm 到 282 μm 内接近线性,当光纤段数增加时波长漂移量变大.

关键词:可调谐;双波长;旁瓣抑制;蚀刻;声光光栅
中图分类号:TN24;TN25;TN29 **文献标识码**:A **文章编号**:1004-4213(2015)08-0806005-6

Tunable Dual-wavelength Filter Based on Cascaded Acousto-optic Gratings in Diam-etched Fiber

JIA Jie, FENG Xuan-qi, ZHANG Yao, QI Xin-yuan, HE Qing-li, BAI Jin-tao
(*Department of Physics, Northwest University, Xi'an* 710069, *China*)

Abstract: Cascaded diam-etched fiber was studied to realize the dynamic manipulation of dual-wavelength filter. Utilizing the coupled-mode theory and segmented transfer matrix method, the theoretical derivation and simulation calculation were carried out. A new type of tunable dual-wavelength filter was studied based on cascaded Acousto-Optic Gratings (AOGs) in diam-etched fiber. The side lobe suppression effect of diam-etched AOGs in the transmission spectra was analyzed. The results show that optical fiber etching method can effectively suppress the side lobe effect, the side lobe ratio can be decreased from 0.265 to 0.031; The dual-wavelength filter works symmetrically and efficiently with tunable frequency spacing by adjusting the fiber length. When the fiber length increases, left resonant wavelength peak decreases and right resonant wavelength peak increases. The wavelength of the dual wavelength filter tunable adjusted by the frequency of the acoustic signal and the number of segments of the fibers, the dual-wavelength increases with the acoustic wave, and approximately linearly between 270 μm to 282 μm, the wavelength shift enlarges with the number of fiber segments increasing.

Key words: Tunable; Dual-wavelength; Side lobe suppression; Diam-etched; Acousto-optic grating
OCIS Codes: 050.2770; 230.1040; 230.7408; 060.4005

0 Introduction

Dual-wavelength filters have been attracted extensive attention in the applications of wavelength division multiplexing, optical communication networks and optical sensor systems[1]. Various techniques have

Foundation item: Scientific Research Plan of Shaanxi Province Education Department(No. 14JK1763)
First author: JIA Jie (1989—), female, M. S. degree candidate, mainly focuses on fiber grating laser technology. Email: jiajie0621@foxmail.com
Supervisor(Contact author): FENG Xuan-qi(1966—), male, lecturer, M. S. degree, mainly focuses on fiber laser. Email: fengxq@nwu.edu.cn
Received: Mar. 08, 2015; **Accepted**: May. 21, 2015

been proposed to realize switching between wavelengths as well as controlling wavelength spacing independently. Different types of Fiber Bragg Grating (FBG) have been used to perform wavelength filter. These include cascaded FBG[2], inline topology FBGs[3], FBGs written in a high birefringent fiber[4], long-period fiber gratings[5] and so on. Stable multi-wavelength operation of Erbium-Doped Fiber Ring Laser (EDFL) with tunable wavelength spacing has also been achieved by using technologies, such as a segmented all-Polarization Maintained (PM) fiber ring resonator[6], spacing-tunable multi-wavelength comb filters[7] and chirped FBGs[8].

Recently, there is an increasing interest in all fiber Acousto-Optic (AO) tunable filters due to their remarkable characteristics of narrow bandwidth, low crosstalk, wide and fast wavelength tuning, low polarization dependence and variable attenuation with simple electric control[9]. These characteristics based on the acoustically induced mode coupling have been applicated into notch filters[10], frequency shifters[11], add/drop channel coupler[12]. However, these filters still suffers from intrinsic side lobes on both sides of the main filtering band. Up to date, several approaches have been proposed to suppress the side lobes in all-fiber flexural mode AOTFs[13].

In this paper, we demonstrate a tunable dual-wavelength filter with AO mode coupling in fiber. In particular, the strength of side lobes is completely minimized in transmission spectra of diam-etched AO Gratings(AOGs). Our studies provide a simple way to realize the dynamic manipulation of dual-wavelength filter.

1 Theory and analysis

As is well-known the efficiency of the mode coupling provided by the flexural acoustic wave can be studied with the coupled mode theory, while the details of the acoustic-wave propagation in a fiber has been well described in Ref. [14]. Here we consider the coupling between two forward propagating modes in a uniform AOG. $E_1(z)$ and $E_2(z)$ are the electric fields of the modes LP_{01} and LP_{0m}, which can be expressed by $E_1(z)=A_1\exp(i\beta_1 z)$ and $E_2(z)=A_2\exp(i\beta_2 z)$ respectively. β_1 and β_2 are the propagation constants of the two modes respectively. In a perfect fiber without any perturbation, the mode amplitudes are constants. Referring to Fig. 1(b), we assume a sinusoidal index perturbation in the z direction

$$\Delta n^2(z)=d(z)(n_1^2-n_2^2)\frac{1}{2}(e^{-iKz}+e^{iKz}) \quad (1)$$

where n_1, n_2 are the refractive indices of the core and cladding respectively, and K is the wave vector related to the AO-grating period Λ by $K=2\pi/\Lambda$. Ideally, the etched depth d of the fiber obeys

$$d(z)=\alpha\exp\left[-\ln(2)\left(\frac{2(z-L/2)}{\gamma L}\right)^4\right] \quad (2)$$

$L=8$ cm is the total length of the AOGs. $\alpha=0.3$ is a constant. γL is the FWHM of the 4th order function and $\gamma=0.9$. α is the maximum refractive index modulation, γ is gradient parameter. Obviously, it is very difficult to make all the fiber etched depths match exactly the continuous Gaussian distribution shown in Fig. 1(a). Therefore, we use discrete model to approach the idea case

$$\Delta n_m^2(z)=\sum_1^{N_s} d_m(z)(n_1^2-n_2^2)\frac{1}{2}(e^{-iKz}+e^{iKz})$$

where $d_m(z)$ is constant for each segments and m is the number of the segments. The relative diam-etched depth parameter $d_m(z)$ of four (Solid) and ten (Dash) AOG segments according to Gaussian distribution is shown in Fig. 1(a). The dot-dashed line is the continuous Gaussian distribution. In the discrete model the midpoint of each segments are taken from the continuous Gaussian curve as the values of whole segment.

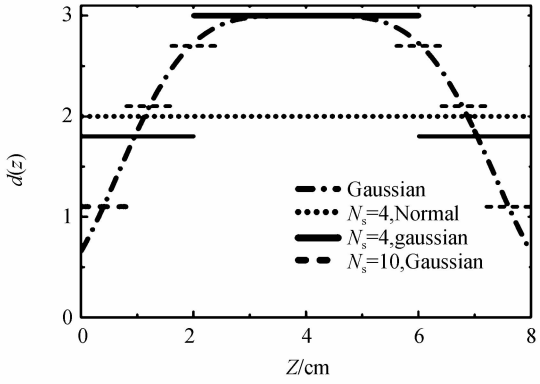

(a) The relative diam-etched depth of AOG

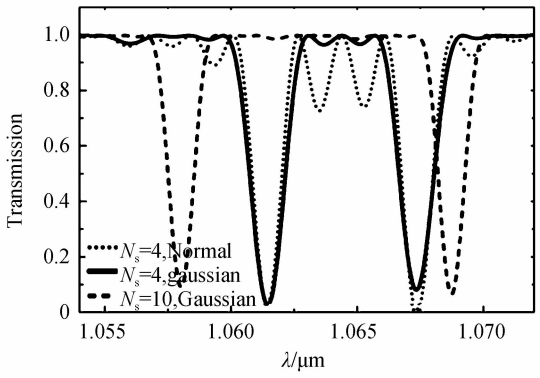

(b) The transmission spectra of the dual-wavelength filter

Fig. 1 The transmission spectra of diam-etched AOG

As a result, the mode amplitudes A_1 and A_2 are dependent on the distance of propagation z. The Fourier expansion consists only of the fundamental orders, and all higher order Fourier components are zero. Thus, the coupling coefficient is given by

$$k(z)=\frac{\omega}{8}\varepsilon_0(n_1^2-n_2^2)d(z)\int_0^r E_1^*(x)E_2(x)\mathrm{d}x \quad (3)$$

We note that the coupling coefficient is directly proportional to the depth of the index modulation $d(z)$. Our project describes a more general case of index gratings in which both the amplitude of the index modulation and the periodicity varies with acoustic wave. When the coupled modes propagate in the same direction, the $+z$ direction. The coupled equations turn into

$$\begin{aligned}\frac{\mathrm{d}}{\mathrm{d}z}A_1 &= -\mathrm{i}kA_2(z)\mathrm{e}^{\mathrm{i}\Delta\beta z}\\ \frac{\mathrm{d}}{\mathrm{d}z}A_2 &= -\mathrm{i}k^* A_1(z)\mathrm{e}^{-\mathrm{i}\Delta\beta z}\end{aligned} \tag{4}$$

where the coupling constant $\kappa(z)$ is related to $d(z)$, is a function of N_s, and the phase mismatch $\Delta\beta$ is a function of $\Lambda(f)$ and is given by

$$\Delta\beta = 2\beta - \frac{2\pi}{\Lambda(f)} \tag{5}$$

where $\Lambda = (\pi R C_{\mathrm{ext}}/f)^{1/2}$, $C_{\mathrm{ext}} = 5760$ m/s is the speed of the acoustic wave in silica, f is the frequency of the acoustic wave, R is the fiber radius.

The transmission coefficient $T = A_2(L)/A_1(0)$ can be obtained by using matrix method. In cascaded grating, we may treat each segment as a simple index grating.

We define the actual electric field of the wave as

$$\begin{aligned}a(z) &= A_1(z)\mathrm{e}^{-\mathrm{i}\beta z}\\ b(z) &= A_2(z)\mathrm{e}^{\mathrm{i}\beta z}\end{aligned} \tag{6}$$

Then the general solutions of the coupled equations for a simple index grating (with constant s and Λ) can be written in a matrix form as

$$\begin{bmatrix}a(z)\\ b(z)\end{bmatrix} = \begin{bmatrix}\cosh sz - \mathrm{i}\dfrac{\Delta\beta}{2s}\sinh sz & -\mathrm{i}\dfrac{k}{s}\sinh sz\\ -\mathrm{i}\dfrac{k^*}{s}\sinh sz & \cosh sz + \mathrm{i}\dfrac{\Delta\beta}{2s}\sinh sz\end{bmatrix}\begin{bmatrix}a(0)\\ b(0)\end{bmatrix}$$

where $a(0)$ and $b(0)$ are the field amplitudes at $z=0$. For cascaded grating, we may treat each segment as a simple homogeneous index grating. We define a matrix

$$[F_n] = \begin{bmatrix}\cosh s_n z_n - \mathrm{i}\dfrac{\Delta\beta}{2s_n}\sinh s_n z_n & -\mathrm{i}\dfrac{k}{s_n}\sinh s_n z_n\\ -\mathrm{i}\dfrac{k^*}{s_n}\sinh s_n z_n & \cosh s_n z_n + \mathrm{i}\dfrac{\Delta\beta}{2s_n}\sinh s_n z_n\end{bmatrix}$$

for the nth segment, where z_n is the length of the nth segment, κ_n is the corresponding coupling coefficient for the nth segment, $s_n = \sqrt{k_n^2 - (\Delta\beta_n/2)^2}$.

We now combine the all the matrices into one and obtain

$$\begin{bmatrix}a_N\\ b_N\end{bmatrix} = \prod_{n=1}^{N_s}\begin{bmatrix}\mathrm{e}^{-\mathrm{i}(\beta_1+\beta_2+\pi/\Lambda)L_g} & 0\\ 0 & \mathrm{e}^{-\mathrm{i}(\beta_1+\beta_2-\pi/\Lambda)L_g}\end{bmatrix}\cdot [F_n]\begin{bmatrix}a_0\\ b_0\end{bmatrix} = \begin{bmatrix}F_{11} & F_{12}\\ F_{21} & F_{22}\end{bmatrix}\begin{bmatrix}a_0\\ b_0\end{bmatrix} \tag{7}$$

where L_g is the length of unetched connection fiber (g_1, g_2 and g_3). F represents the action of the whole system on the input beam. F_{11}, F_{12}, F_{21} and F_{22} are the matrix elements of the compound transfer matrix F.

If there is only one mode excited when the light enters the coupling region, the acousto-optic grating transmission can thus be written in term of the matrix elements of the transfer matrix

$$T = \left(\frac{b_N}{a_0}\right)_{b_0=0} = \frac{F_{21}}{F_{11}} \tag{8}$$

Obviously, one can tune the transmission by changing the F_{21} and F_{11}. While F_{21} and F_{11} are determined by the L_g, the acoustic wavelength $\Lambda(f)$ and number of segments of the fibers N_s. The variation of L_g changes the initial phase of each segments, which has a great influence on the peak transmission of the dual-wavelength. The flexural acoustic wavelength $\Lambda(f)$ is generated by using a piezoelectric transducer driven by a Radio Frequency (RF) signal f. Therefore it permits independent tuning of the central wavelength of the dual-wavelength. Eq. 7 indicates N_s reflects the feature of AOGs. In a word, one can adjust the above parameters simultaneously or separately. The further studies based on these analysis are proceeded in the following section.

2 Result and discussion

In this section, we numerically study the transmission of our system with Matlab. It is well known that when a AOG is reduced to be thin by chemical etching, the diam-etched AOG is much more sensitive to environmental change than the regular AOG with a normal cladding layer. When the acoustic wave propagates along the diam-etched AOG, a periodic modulation of the refractive index is produced with a period of hundreds of micrometers in the core of the fiber, and such a core refractive index modulation would distributed according to the depth of the etched AOG.

Schematic of the four segments dual-wavelength filter is shown in Fig. 2. The dual-wavelength filter can be continuous tuned efficiently by adjusting the number of the diam-etched AO segments (N_s), the fiber length (L_g) and the frequency of the acoustic wave ($\Lambda(f)$), respectively. Fig. 2(a) is the schematic of the dual-wavelength filter with four diam-etched AOGs as an example. The uniform fiber had a step index of $n_1 = 1.44921$ and $n_2 = 1.44403$, with a core diameter of $D_{\mathrm{co}} = 5.0$ μm and a cladding diameter of $D_{\mathrm{cl}} = 125$ μm. The outer diameter of the AOGs was etched down to different radius by the hydrofluoric acid according to Gaussian distribution. In this four segments case, the etched depth of G_1, G_2, G_3 and G_4 is shown in Fig. 2

(b). We assumed that $d_1(z)=0.18$, $d_2(z)=0.3$ are determined by the diam-etched depth of AOG, as shown in Fig. 1(a). The length of each etched segments was $L_G=20$ mm, and the length of the unetched connection part of the filter g_1, g_2 and g_3 was $L_g=10$ mm. With this configuration, the side lobe suppression is present in Fig. 1(b). The dot curve denotes the transmission spectrum of four equal diam-etched ($d(z)=0.3$) AOGs. When the diam-etched depths related parameter $d(z)$ of these segments are as those shown in Fig. 1(a), the side lobes between the dual-wavelength are practically eliminated Fig. 1(b) (Solid &Dash). The transmission turns out to be smooth curves without small notches in spite of two passbands in which the center frequencies have been filtered. Sidelobe ratio decreased from 0.265 to 0.031. Filter's 3dB filter width, wavelength tuning range, insertion loss, crosstalk does not change.

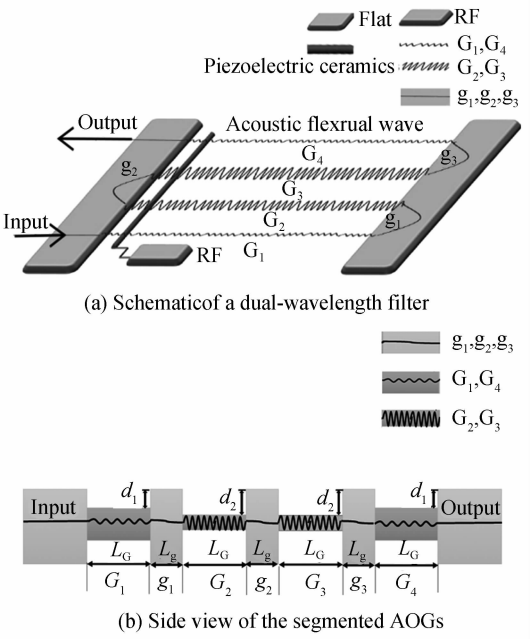

Fig. 2 Structure diagram of a dual-wavelength filter

From Eq. (4) and Eq. (7), it is clear that there are three parameters can be adjusted to manipulate the transmission of the dual-wavelength filter. Firstly, the stability of the passbands of the dual-wavelength is explored in Fig. 3 and Fig. 4. According to the numerical results shown in Fig. 3, for three different lengths, it is found that the central wavelength of the two peaks as a function of length of unetched connection fibers L_g. Fig. 4 shows how the fiber length affects the stability of the peaks. One sees that the left peak of the dual-wavelength coincides with the right peak, which means that the peak of dual-wavelength could be adjusted by choosing optimal L_g (intersection). Meanwhile, the spectral central wavelength of dual-wavelength is proportional to L_g.

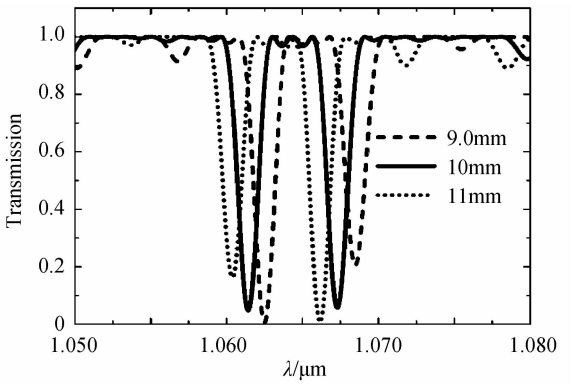

Fig. 3 Transmission of acousto-optic filter for three length of unetched connecting fiber L_g

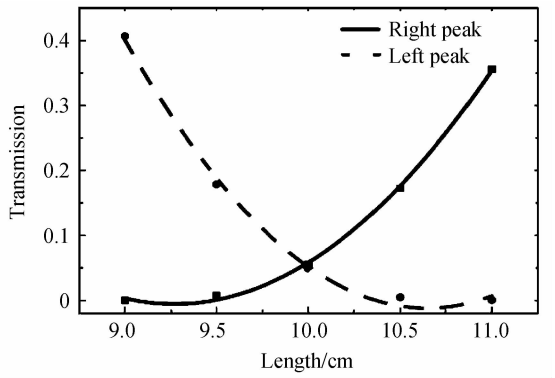

Fig. 4 The right and left peak transmissions with the change of fiber length

The tuning range of the dual-wavelength is showed in Fig. 5 and Fig. 6. Dual-wavelength shifts as a

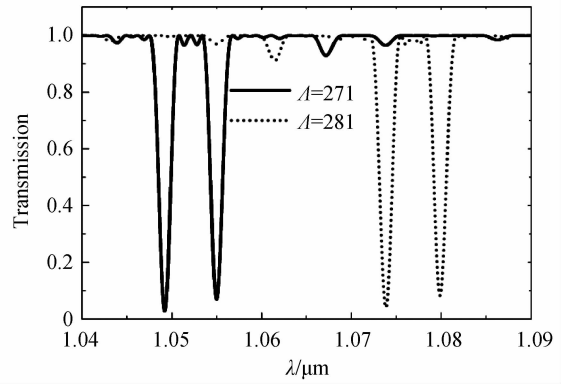

Fig. 5 Transmission spectra of different Λ fiber filter

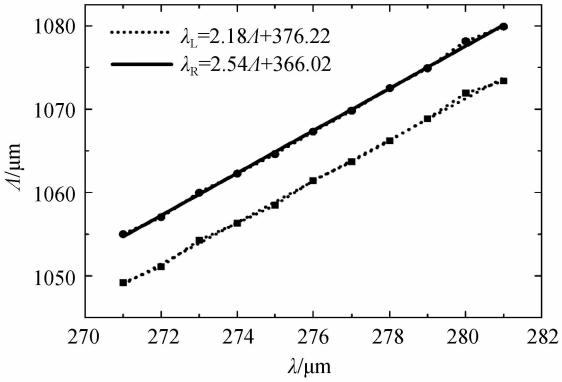

Fig. 6 λ_R and λ_L tunability by the wavelength Λ of the acoustic wave

function of AO grating period induced by acoustic frequency f, which was limited by the acoustic transducer. An improved design of the transducer can extend the tuning range. Here, the solid line shows the spectrum at $\Lambda=271$ μm and the red dotted line shows at $\Lambda=281$ μm. The center wavelength shift of the dual-wavelength as a function of the grating period. Fig. 6 shows a nearly linear relationship between the central wavelength of the dual-wavelength and the wavelength Λ of the acoustic wave.

The results of the span of the dual-wavelength filter are shown in Fig. 7 and Fig. 8. The span of the dual-wavelength increases with number of AOG segments when the total length of the AOGs is $L=8$ cm. Fig. 7 shows the typical spectra of dual-

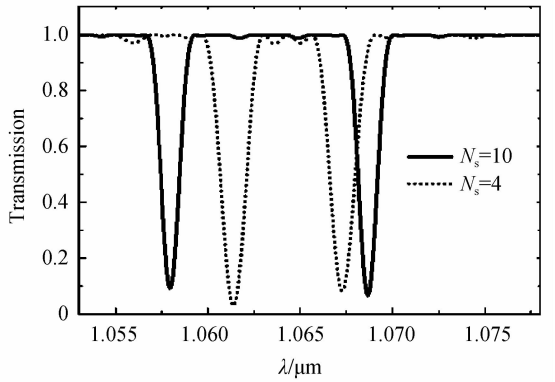

Fig. 7 Transmission spectra of different N_s fiber filter

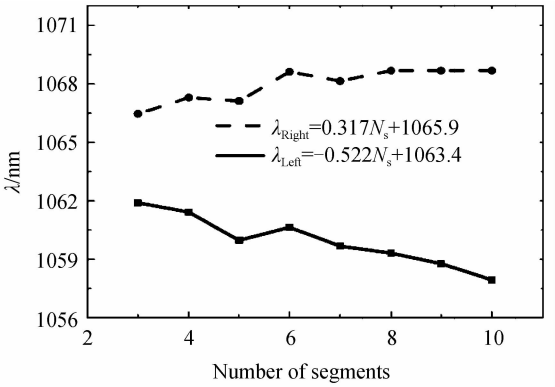

Fig. 8 The span of the dual-wavelength with the change of the number of fiber segments

wavelength when the number of segments was four (dotted line) and ten (solid line), respectively. Furthermore, we find that the side lobes between the dual-wavelength can be eliminated by properly distributing the diam-etched AOGs. This technique of suppressing side lobes for AOG can be easily realized.

The dependence of the dual-wavelength spacing with different number of segments while the total length remains unchanged, is shown in Fig. 8. Obviously, the wavelength shift increase with respect to the number of segments. We note that the span won't get bigger indefinitely. When L_G is close to L_g, that is to say, N_s is more than 10 segments. Considering the mechanical properties of the AOG, the wavelength spacing can tune from 3.6 nm ($N_s=3$) to 11.4 nm ($N_s=10$).

It should be noted here that our study has examined only under ideal conditions, it is important to consider the effects of various perturbations such as temperature fluctuation, fiber bending or twist, and axial strain on the device performances for the real situations. Despite these preliminary character, our study clearly indicates the tunability of the dual-wavelength filter, and has potential applications in the design of laser, filters and sensors.

3 Conclusion

We have theoretically and numerically studied the transmission of the tunable dual-wavelength filter based on cascaded acousto-optic gratings in diam-etched fiber. Theoretical studies show that the transmission is determined by the length of each fiber segment, the frequency of the acoustic wave and the number of the fiber segments. The numerical results demonstrate that the stability of the dual-wavelength could be adjusted. The central wavelength of dual-wavelength are proportional to the frequency of the acoustic wave. And the wavelength span increases with the number of the AOG segments. Our studies provide a simple way to realize the dynamic manipulation of dual-wavelength filter while keeping the side lobes in the filter spectrum is suppressed efficiently. The demonstrated tunable dual-wavelength filter provides a new way to adjust the dual-wavelength simultaneously and has promising applications in the laser and optical communications.

References

[1] YANG Xiu-feng, GE Chun-feng. Dual wavelength narrow line-width fiber grating ring cavity laser[J]. *Acta Photonica Sinica*, 1998, **27**(5): 438-440.

[2] MA Jun-shan, GENG Jian-xin. A dual-mode external cavity laser diode with cascaded fiber Bragg gratings [J]. *Acta Photonica Sinica*, 2001, **30**(8): 994-997.

[3] TALAVERANO L, ABAD S, JARABO S, *et al*. Multiwavelength fiber laser sources with Bragg-grating sensor multiplexing capability [J]. *Journal of Lightwave Technology*, 2001, **19**(4): 553-558.

[4] HEMANDEZ J, KOZLOV V, CARTER A, *et al*. Fiber laser polarization tuning using a Bragg grating in a Hi-Bi fiber[J]. *Photonics Technology Letters*, 1998, **10**(7): 941-943.

[5] XU Xin-hua. Linearly chirped long period gratings used for EDFA gain flattening[J]. *Acta Photonica Sinica*, 2009, **38**(8): 2063-2065.

[6] YU Kan, LIU Wen. A novel three-port band pass tunable filter[J]. *Acta Photonica Sinica*, 2009, **38**(3): 670-673.

[7] HUO Lei, ZENG Xiao-dong, FENG Zhe-jun. Non-reciprocity of collinear acousto-optic tunable filter[J]. *Acta Photonica Sinica*, 2011, **40**(8): 1149-1153.

[8] YANG J. Tunable multi-wavelength combined linear-cavity

fiber laser source with equally changed wavelength spacing[J]. *Optics and Laser Technology*, 2002, **34**(8): 599-604.

[9] PARK H S, SONG K Y, YUN S H. All-fiber wavelength-tunable acoustooptic switches based on intermodal coupling in fibers[J]. *Journal of Lightwave Technology*, 2002, **20**(10): 1864-1868.

[10] ZHANG W, GAO F, BO F. All-fiber acousto-optic tunable notch filter with a fiber winding driven by a cuneal acoustic transducer[J]. *Optics Letters*, 2011, **36**(2): 271-273.

[11] KIM B, BLAKE J, ENGAN H. All-fiber acousto-optic frequency shifter[J]. *Optics Letters*, 1986, **11**(6): 389-391.

[12] ZHANG W, HUANG L, GAO F. Tunable add/drop channel coupler based on an acousto-optic tunable filter and a tapered fibe[J]. *Optics Letters*, 2012, **37**(7): 1241-1243.

[13] LEE K J, HWANG I K, PARK H C. Sidelobe suppression in all-fiber acousto-optic tunable filter using torsional acoustic wave[J]. *Optics Express*, 2010, **18**(12): 12059-12064.

[14] ENGAN H E, KIM B Y, BLAKE J N. Propagation and optical interaction of guided acoustic waves in two-mode optical fibers[J]. *Journal of Lightwave Technology*, 1988, **6**(3): 428-436.